**Brookhaven National Laboratory**

**MEMORANDUM**

DETECTOR RHIC GROUP

Date: 06/19/96

To: S. Musolino

From: A.J. Stevens ajs

Subj.: More on Survey Shafts

The analysis of the survey shafts in the vicinity of the first sextant test was circulated to the RSC and you are one of the few who returned the summary of the analysis with "accept" indicated. A part of that analysis stated that the estimated *total* dose *beside* the shafts relevant to both the first sextant test and the collider was under our 160 mrem. criteria. The details of the components are given in the table below.

| Shaft dia. | 1-Leg Laby. dose (mrem) | DOSEXIT dose (mrem) | No-hole dose (mrem) | Total (mrem) | Total beside shaft (mrem) |
|---|---|---|---|---|---|
| 12 inch | 195 | 75 | 64 | 334 | 91 |
| 18 inch | 314 | 285 | 81 | 680 | 141 |

The last column is one tenth of the 1-Leg + DOSEXIT dose plus the No-hole dose.

The recent memorandum on the excess dose from generic survey shafts did not include the No-hole contribution, but I did not forget this contribution in applying the analysis to a specific case. The excess dose for the 12 inch case in the table totals 270 mrem, not the 220 mrem stated for the generic 12 inch hole in the memorandum. This is because this particular survey shaft is not located in the standard tunnel enclosure, but in an "expanded" section, and the slight difference in geometry has been taken into account.

**Brookhaven National Laboratory**

## MEMORANDUM

DETECTOR RHIC GROUP

Date: 06/14/96

To: S. Musolino

From: A.J. Stevens AJS

Subj.: Updated Evaluation of Straight-Through Penetrations

This memorandum is an update to a memorandum dated 11/04/92 whose subject was "Straight-Through Penetration Evaluations." That memorandum estimated the dose at the exits of survey shafts at RHIC by using calculations performed by Andy Van Ginneken and gave an upper limit for the dose at the exit of the large holes which exist at some places (e.g., 6 o'clock) for cryogenics bypasses.

Two changes have occurred related to the survey penetrations. The first is that most (but not all) penetrations are 12 inches in diameter rather than 18 inches previously assumed. Secondly, the technique for evaluation has evolved. We now consider dose exiting the tunnel to have two components: (1) low energy neutrons which stream through the penetration, and (2) a "punch-through" contribution. The former is estimated by applying the single leg labyrinth formula of Goebel and the normalization of Gollon[1], whereas the latter comes from the DOSEXIT program.[2]

Numerically, I consider here two "prototypical" survey shafts, a 12 inch dia. which extends 2 ft. above the berm and an 18 inch dia which extends 1 ft above the berm. The total lengths of the penetrations are 515 cm. and 485 cm. respectively. These are penetrations actually existing in the region between 6 o'clock and 4 o'clock. The star density in soil around the tunnel for faults by 250 GeV/c protons is given by:[3]

$$\text{Star Density (stars/cc-proton)} = 6.6 \times 10^{-6} \times \frac{e^{-d/.67}}{R^2}$$

Using .85 times the above at R=1.88m and $d$=0 gives the entrance dose (with the usual dose to rem conversion multiplied by 2) for the first leg labyrinth formula, and the formula is integrated into dosexit.

The results are given in the table below.

**Dose/250 GeV proton for Survey Shafts**

| Diameter (inches) | Dose (Laby. Form.) (rem/p) | Dose (DOSEXIT) (rem/p) | Dose - Total (rem/p) |
|---|---|---|---|
| 12 | $6.88\times10^{-15}$ | $1.25\times10^{-14}$ | $1.94\times10^{-14}$ |
| 18 | $2.76\times10^{-14}$ | $2.53\times10^{-14}$ | $5.29\times10^{-14}$ |

The $5.29\times10^{-14}$ rem/p compares to $4.0\times10^{-14}$ rem/p in the previous memorandum which is excellent agreement. No survey shafts yet identified are near the high $\beta$ quads which means that the design basis accident at 4 times design intensity corresponds to the loss of $1.14\times10^{13}$ protons giving either 220 mrem (12 inch) or 600 mrem (18 inch). Since the dose should be a factor of 10 down for a person standing beside the shaft,[3] these are not a problem if "fenced" properly.

The previous memorandum also estimated the dose at the exit of a 5 ft. long cryogenics penetration (which is near a high $\beta$ quad) to be less than 25 rem. In reviewing the previous memorandum, I believe the scale factor used because of the presence of Fe (which is "thin" in Gollon's nomenclature) was overestimated. A factor of 1.5 beyond the CASIM dose should be quite sufficient which reduces the estimate to about 12 rem. As mentioned in the previous memorandum, this assumes an empty penetration and thus is still an upper limit.

## References


1. P.J. Gollon, "Shielding of Multi-Leg Penetrations into the RHIC Collider," AD/RHIC/RD-76 (1994).

2. J.R. Preisig and A.J. Stevens, "Estimation of Neutron Punch-Through in Circular Shielding Penetrations," AD/RHIC/RD-81 (1994).

3. A.J. Stevens, "Radiation Field in the Vicinity of the Collider Center," AD/RHIC/RD-77 (1994).

**Brookhaven National Laboratory**

# MEMORANDUM

Date: 11/04/92

To: S. Musolino

From: A.J. Stevens *ajS*

Subject: Straight-Through Penetration Evaluations

Andy Van Ginneken has, as you know, performed a reasonably detailed evaluation of the dose equivalent at the exit of the survey shafts in the collider tunnel. I summarize here the result of that evaluation in order to compare it with a simple CASIM calculation I have recently performed which was intended to obtain an **upper limit** on the dose which might emerge from the large holes represented by the penetrations intended to carry the cryogenic plumbing across experimental halls.

Andy's result was obtained for 100 GeV/c protons and used the "normal" conversion factors for dose per neutron and dose per CASIM star. Since we are designing for twice the dose per neutron, I take the dose equiv. at the exit of the survey shaft to be twice the value given by Andy, or $< 1.8 \times 10^{-14}$ rem/p. This estimate is the sum of 4 terms: (1) the dose from (carried by) high energy (>50 MeV) particles originating near the shaft, (2) low energy neutrons coming from the "target" (a magnet), (3) direct dose from high energy particles coming straight through the shaft, and (4) a CASIM dose estimated as if the penetration were absent. Adding these components results in some "double counting" which is the reason I quote Andy's result as an upper limit.

Before describing the cryo. penetration calculation, I note the fact that at least some survey shafts also exist in the Transfer Line. I have scaled Andy's components (1), (3), and (4) by $E^{.8}$ and (2) by E to obtain a limit of $6 \times 10^{-15}$ rem/p in this case. A fault of 2 AGS pulses ($4.8 \times 10^{12}$ 28 GeV protons) gives 24 mrem. Since the earth berm is nominally the same in both Transfer Line and collider tunnel, I do not believe that further sophistication is required unless the shaft is pointed directly at the Transfer Line magnets which I do not believe is the case, although this point should be checked.

The survey shafts are offset with respect to the tunnel center line and relatively small ( ~ 18" dia.). Neither of these helpful characteristics apply to the cryo. bypass shafts.

I have performed two CASIM calculations, both quite simple, related to this penetration. Both were performed at 250 GeV and assume scrapng on one of the high $\beta$ quads (Q3). The first, performed simply to observe the result, assumes **no berm at all**. The star density was calculated in a shell located at a radius of 656 cm. with respect to the beam center line. The result, expressed in dose equiv. as above, was:

$$5.8 \times 10^{-12} \cdot f \text{ rem/p}.$$

where an enhancement factor "f" is required because the CASIM star density to dose conversion assumes some hydrogeneous material (such as soil) exists. For pure Fe, Stevenson[1] has estimated f = 5.

To simulate a large, but **finite** hole, I perform a calculation similar to the above but with a berm which begins at R = 264 cm. which is the approximate distance from the beam line to the roof in an "expanded" tunnel section. A 150 cm. long "gap" in the berm is assumed to exist between 264 and 656 cm. which is moved along the beam direction until the worst case star density at R= 656 cm. is found. The result of this calculation is:

$$3.6 \times 10^{-13} \cdot f \text{ rem/p}.$$

In this case it is not clear what value that the enhancement factor should take since part of the dose in the shell comes directly from the magnet and part through the earth region which partially shields the hole. Since the star density is reduced from the no-berm case by over an order of magnitude, one would assume that **most** of the dose comes through some earth, so f should presumably be smaller than 5. I will allow f = 3 which is likely quite conservative. In this case, dose $< 1.08 \times 10^{-12}$ rem/p. For a complete fault of $2.28 \times 10^{13}$ protons, the dose at the shaft exit is then < 25 rem.

In real life, of course, the cryo. shaft is partially occupied with material which greatly reduces the estimate given here. Although the estimate for this penetration is much larger than for the survey shaft, Andy's result is itself a cause for concern. Applying the same scaling as described above to 250 GeV gives $4.0 \times 10^{-14}$ rem/p. For shafts near high $\beta$ quads or one of the other objects near the limiting aperture, a full fault of $2.28 \times 10^{13}$ protons gives 910 mrem. To reduce this to 160 mrem would require the equivalent of almost 4 ft. of earth.

1. G.R. Stevenson, "Dose Equivalent per Star in Hadron Cascade Calculations",CERN Report TIS-RP/173, May, 1986.

Fermilab

Fermi National Accelerator Laboratory
P.O. Box 500 • Batavia, Illinois • 60510

October 21 1992

To: A. J. Stevens
RHIC, BNL

From: A. Van Ginneken

Re: CASIM Calculation for RHIC Tunnel Penetration

Herewith some results of the calculation you requested in your letter of October 9 regarding dose outside a tunnel penetration. To suit this particular version of CASIM some alterations were necessary from the geometry you proposed. (The penetration version is more restrictive in this regard than just plain CASIM.) Primarily, geometry and beam loss must be cylindrically symmetric and the geometry must also have translation symmetry. To this end the magnet is replaced with a solid cylinder 10 cm in radius which is roughly the thickness of the outer shell you propose and is also close to a worst case target of this kind. The solid cylinder results in a more compact source and thus in a 'worse case' than the hollow cylinder. This cylinder runs the entire length of the tunnel and is placed at the center of a tunnel with a 188 cm radius. The represents (to the nearest cm) the distance from magnet center to tunnel wall at the center of the penetration. The tunnel is circular and not horseshoe-shaped. I chose the tunnel to be 10 m long. It needs to be long enough to contain the maximum of the dose outside the tunnel (which is calculated as a function of z) while still allowing it to be clearly resolved.

The basic parameters of the calculation are then the above target and tunnel dimensions, the angle between penetration and radial vector (0.659 rad), the cross sectional area of the penetration (1662 $cm^2$), and of course the 100 GeV incident proton energy. There is also the length of the penetration which is taken as 455 cm. The calculation actually presents results for five different lengths (starting at 405 cm and incremented by 50 cm) to give some idea of the dependence of dose on length of the penetration.

As can be seen from the results there are three principal contributions to the dose on top of the penetration: (1) CASIM type particles which originate in the tunnel wall around the penetration and then take advantage of it to escape the shield (labeled 'high energy contribution'). It is assumed that these particles are accompanied by the usual low energy equilibrium neutrons when converting flux (or stars) to dose. (2) A low energy contribution due mainly to low energy neutrons which originate in the target. During the Monte Carlo the number of such neutrons produced as a function of location in the target is kept track of. At the conclusion their flux at the mouth of the penetration is estimated and they are then propagated through it using the empirical rules for labyrinth transmission. (3) The component labeled 'CASIM without penetration' refers to what is expected if no penetration were present. This explores the other patways by which the particles can escape the shield. The fourth component ('direct') is what comes up through the entire penetration after bouncing around in the tunnel. Its estimate is somewhat limp here but the low value suggests that this may be neglected anyway. In reality these particles would come up from the floor which is some 171 cm from the magnet center, not 188 cm as in the calculation. The floor presents a plane surface while in the calculation assumes it is cylindrical. The distance from floor to penetration is about 275 cm from your sketch versus about 295 cm in the CASIM run. Nonetheless these numbers are close enough so that a negligible result here should hold for a more realistic estimate as well. This can be done, by the way, only it gets more complicated. Incidentally, combining these components by just adding them up may well result in some 'double counting'. But for the most part they are independent. Adding components (1) and (3) may raise the most suspicion. But it is known that (in a problem like this one) most of (1) results from particles originating from stars located at relatively small radii which—if there were no penetration—would hardly contribute.

I am enclosing the results which include a breakdown by component. I don't know if this brings good news or bad. Also included is a copy of your sketch on which I made some notations that you might want to check out along with some of the numbers provided above. Let me know if you need further information.

encl.

dose rate at surface (rem/inc.p) as a function of distance along the beam (z,down in cm)
for tunnel-to-surface penetration of cross sectional area= 1662.00 cm2 angle w/r to beam direction= 1.57 radians
projected angle w/r to radial direction= 0.66 radians
for different lengths of penetration (in cm, across)

high energy contribution

| | 405.000 | 455.000 | 505.000 | 555.000 | 605.000 |
|---|---|---|---|---|---|
| 10.00 | 2.94E-15 | 2.70E-16 | 1.51E-16 | 9.73E-17 | 6.73E-17 |
| 30.00 | 3.35E-15 | 3.75E-16 | 2.17E-16 | 1.43E-16 | 1.00E-16 |
| 50.00 | 4.34E-15 | 6.04E-16 | 3.58E-16 | 2.38E-16 | 1.68E-16 |
| 70.00 | 6.31E-15 | 9.15E-16 | 5.46E-16 | 3.65E-16 | 2.58E-16 |
| 90.00 | 9.50E-15 | 1.34E-15 | 8.07E-16 | 5.41E-16 | 3.84E-16 |
| 110.00 | 1.34E-14 | 1.87E-15 | 1.13E-15 | 7.57E-16 | 5.39E-16 |
| 130.00 | 1.53E-14 | 2.30E-15 | 1.39E-15 | 9.39E-16 | 6.69E-16 |
| 150.00 | 1.74E-14 | 2.72E-15 | 1.66E-15 | 1.12E-15 | 8.02E-16 |
| 170.00 | 2.20E-14 | 3.29E-15 | 2.00E-15 | 1.35E-15 | 9.67E-16 |
| 190.00 | 2.48E-14 | 3.76E-15 | 2.29E-15 | 1.55E-15 | 1.11E-15 |
| 210.00 | 2.74E-14 | 4.08E-15 | 2.48E-15 | 1.68E-15 | 1.20E-15 |
| 230.00 | 3.03E-14 | 4.30E-15 | 2.60E-15 | 1.76E-15 | 1.25E-15 |
| 250.00 | 3.24E-14 | 4.38E-15 | 2.64E-15 | 1.78E-15 | 1.27E-15 |
| 270.00 | 3.23E-14 | 4.44E-15 | 2.69E-15 | 1.82E-15 | 1.30E-15 |
| 290.00 | 3.24E-14 | 4.49E-15 | 2.71E-15 | 1.83E-15 | 1.31E-15 |
| 310.00 | 3.40E-14 | 4.42E-15 | 2.65E-15 | 1.79E-15 | 1.27E-15 |
| 330.00 | 3.55E-14 | 4.38E-15 | 2.61E-15 | 1.75E-15 | 1.26E-15 |
| 350.00 | 3.46E-14 | 4.25E-15 | 2.54E-15 | 1.70E-15 | 1.21E-15 |
| 370.00 | 3.48E-14 | 4.04E-15 | 2.40E-15 | 1.61E-15 | 1.15E-15 |
| 390.00 | 3.56E-14 | 3.91E-15 | 2.31E-15 | 1.54E-15 | 1.09E-15 |
| 410.00 | 3.12E-14 | 3.72E-15 | 2.20E-15 | 1.47E-15 | 1.04E-15 |
| 430.00 | 2.91E-14 | 3.49E-15 | 2.07E-15 | 1.38E-15 | 9.85E-16 |
| 450.00 | 3.42E-14 | 3.46E-15 | 2.03E-15 | 1.35E-15 | 9.56E-16 |
| 470.00 | 3.91E-14 | 3.35E-15 | 1.93E-15 | 1.27E-15 | 8.99E-16 |
| 490.00 | 3.50E-14 | 3.15E-15 | 1.81E-15 | 1.20E-15 | 8.43E-16 |
| 510.00 | 3.17E-14 | 3.03E-15 | 1.75E-15 | 1.15E-15 | 8.14E-16 |
| 530.00 | 2.84E-14 | 2.79E-15 | 1.62E-15 | 1.07E-15 | 7.59E-16 |
| 550.00 | 2.68E-14 | 2.66E-15 | 1.54E-15 | 1.02E-15 | 7.21E-16 |
| 570.00 | 2.77E-14 | 2.57E-15 | 1.47E-15 | 9.70E-16 | 6.82E-16 |
| 590.00 | 2.68E-14 | 2.37E-15 | 1.35E-15 | 8.87E-16 | 6.23E-16 |
| 610.00 | 2.77E-14 | 2.26E-15 | 1.28E-15 | 8.36E-16 | 5.86E-16 |
| 630.00 | 2.40E-14 | 2.02E-15 | 1.15E-15 | 7.57E-16 | 5.32E-16 |
| 650.00 | 1.93E-14 | 1.80E-15 | 1.03E-15 | 6.79E-16 | 4.78E-16 |
| 670.00 | 1.72E-14 | 1.71E-15 | 9.78E-16 | 6.42E-16 | 4.51E-16 |
| 690.00 | 1.86E-14 | 1.64E-15 | 9.38E-16 | 6.16E-16 | 4.33E-16 |
| 710.00 | 1.98E-14 | 1.62E-15 | 9.16E-16 | 6.00E-16 | 4.21E-16 |
| 730.00 | 1.76E-14 | 1.50E-15 | 8.50E-16 | 5.56E-16 | 3.90E-16 |
| 750.00 | 1.38E-14 | 1.31E-15 | 7.51E-16 | 4.93E-16 | 3.47E-16 |
| 770.00 | 1.26E-14 | 1.18E-15 | 6.78E-16 | 4.46E-16 | 3.14E-16 |
| 790.00 | 1.17E-14 | 1.11E-15 | 6.41E-16 | 4.22E-16 | 2.97E-16 |
| 810.00 | 1.39E-14 | 1.10E-15 | 6.28E-16 | 4.13E-16 | 2.91E-16 |
| 830.00 | 1.28E-14 | 1.07E-15 | 6.07E-16 | 3.98E-16 | 2.80E-16 |
| 850.00 | 1.05E-14 | 1.03E-15 | 5.85E-16 | 3.83E-16 | 2.68E-16 |
| 870.00 | 9.59E-15 | 9.87E-16 | 5.61E-16 | 3.61E-16 | 2.54E-16 |
| 890.00 | 8.26E-15 | 8.70E-16 | 5.03E-16 | 3.32E-16 | 2.34E-16 |
| 910.00 | 8.22E-15 | 7.92E-16 | 4.52E-16 | 2.97E-16 | 2.08E-16 |
| 930.00 | 7.26E-15 | 7.25E-16 | 4.13E-16 | 2.70E-16 | 1.89E-16 |
| 950.00 | 7.39E-15 | 7.18E-16 | 4.08E-16 | 2.68E-16 | 1.88E-16 |
| 970.00 | 7.62E-15 | 6.63E-16 | 3.77E-16 | 2.47E-16 | 1.73E-16 |
| 990.00 | 8.56E-15 | 6.01E-16 | 3.37E-16 | 2.20E-16 | 1.54E-16 |

dose rate at surface (rem/inc.p) as a function of distance along the beam (z,down in cm)
for tunnel-to-surface penetration of cross sectional area= 1662.00 cm2 angle w/r to beam direction= 1.57 radians
projected angle w/r to radial direction= 0.66 radians
for different lengths of penetration (in cm, across)

low energy contribution

| | 405.000 | 455.000 | 505.000 | 555.000 | 605.000 |
|---|---|---|---|---|---|
| 10.00 | 4.93E-15 | 3.29E-15 | 2.22E-15 | 1.50E-15 | 1.01E-15 |
| 30.00 | 5.53E-15 | 3.70E-15 | 2.50E-15 | 1.69E-15 | 1.14E-15 |
| 50.00 | 6.07E-15 | 4.06E-15 | 2.74E-15 | 1.85E-15 | 1.25E-15 |
| 70.00 | 6.52E-15 | 4.36E-15 | 2.95E-15 | 1.99E-15 | 1.34E-15 |
| 90.00 | 6.86E-15 | 4.57E-15 | 3.09E-15 | 2.08E-15 | 1.41E-15 |
| 110.00 | 7.03E-15 | 4.66E-15 | 3.15E-15 | 2.13E-15 | 1.44E-15 |
| 130.00 | 7.00E-15 | 4.63E-15 | 3.13E-15 | 2.11E-15 | 1.43E-15 |
| 150.00 | 6.80E-15 | 4.48E-15 | 3.03E-15 | 2.05E-15 | 1.38E-15 |
| 170.00 | 6.47E-15 | 4.24E-15 | 2.86E-15 | 1.93E-15 | 1.31E-15 |
| 190.00 | 6.04E-15 | 3.92E-15 | 2.65E-15 | 1.79E-15 | 1.21E-15 |
| 210.00 | 5.56E-15 | 3.55E-15 | 2.40E-15 | 1.62E-15 | 1.10E-15 |
| 230.00 | 5.06E-15 | 3.17E-15 | 2.14E-15 | 1.44E-15 | 9.77E-16 |
| 250.00 | 4.53E-15 | 2.78E-15 | 1.88E-15 | 1.27E-15 | 8.59E-16 |
| 270.00 | 4.07E-15 | 2.41E-15 | 1.63E-15 | 1.10E-15 | 7.46E-16 |
| 290.00 | 3.58E-15 | 2.08E-15 | 1.40E-15 | 9.48E-16 | 6.42E-16 |
| 310.00 | 3.11E-15 | 1.78E-15 | 1.20E-15 | 8.10E-16 | 5.49E-16 |
| 330.00 | 2.79E-15 | 1.51E-15 | 1.02E-15 | 6.90E-16 | 4.68E-16 |
| 350.00 | 2.50E-15 | 1.28E-15 | 8.65E-16 | 5.86E-16 | 3.98E-16 |
| 370.00 | 2.23E-15 | 1.09E-15 | 7.35E-16 | 4.98E-16 | 3.38E-16 |
| 390.00 | 2.07E-15 | 9.29E-16 | 6.25E-16 | 4.23E-16 | 2.88E-16 |
| 410.00 | 1.87E-15 | 7.92E-16 | 5.32E-16 | 3.61E-16 | 2.46E-16 |
| 430.00 | 1.64E-15 | 6.78E-16 | 4.56E-16 | 3.09E-16 | 2.11E-16 |
| 450.00 | 1.72E-15 | 5.84E-16 | 3.92E-16 | 2.66E-16 | 1.82E-16 |
| 470.00 | 1.73E-15 | 5.06E-16 | 3.38E-16 | 2.30E-16 | 1.57E-16 |
| 490.00 | 1.54E-15 | 4.39E-16 | 2.93E-16 | 1.99E-16 | 1.37E-16 |
| 510.00 | 1.43E-15 | 3.84E-16 | 2.56E-16 | 1.74E-16 | 1.19E-16 |
| 530.00 | 1.37E-15 | 3.37E-16 | 2.24E-16 | 1.53E-16 | 1.05E-16 |
| 550.00 | 1.29E-15 | 2.97E-16 | 1.97E-16 | 1.34E-16 | 9.26E-17 |
| 570.00 | 1.16E-15 | 2.63E-16 | 1.75E-16 | 1.19E-16 | 8.22E-17 |
| 590.00 | 1.07E-15 | 2.35E-16 | 1.55E-16 | 1.06E-16 | 7.32E-17 |
| 610.00 | 1.12E-15 | 2.10E-16 | 1.39E-16 | 9.46E-17 | 6.55E-17 |
| 630.00 | 1.14E-15 | 1.89E-16 | 1.24E-16 | 8.49E-17 | 5.89E-17 |
| 650.00 | 1.02E-15 | 1.70E-16 | 1.12E-16 | 7.65E-17 | 5.31E-17 |
| 670.00 | 8.82E-16 | 1.54E-16 | 1.01E-16 | 6.92E-17 | 4.81E-17 |
| 690.00 | 8.46E-16 | 1.40E-16 | 9.18E-17 | 6.27E-17 | 4.36E-17 |
| 710.00 | 9.20E-16 | 1.28E-16 | 8.35E-17 | 5.70E-17 | 3.98E-17 |
| 730.00 | 1.02E-15 | 1.18E-16 | 7.62E-17 | 5.21E-17 | 3.63E-17 |
| 750.00 | 9.33E-16 | 1.07E-16 | 6.96E-17 | 4.76E-17 | 3.32E-17 |
| 770.00 | 7.70E-16 | 9.79E-17 | 6.36E-17 | 4.36E-17 | 3.04E-17 |
| 790.00 | 7.09E-16 | 9.00E-17 | 5.84E-17 | 4.00E-17 | 2.80E-17 |
| 810.00 | 6.91E-16 | 8.29E-17 | 5.38E-17 | 3.68E-17 | 2.58E-17 |
| 830.00 | 6.26E-16 | 7.64E-17 | 4.96E-17 | 3.40E-17 | 2.38E-17 |
| 850.00 | 5.45E-16 | 7.06E-17 | 4.58E-17 | 3.14E-17 | 2.20E-17 |
| 870.00 | 5.24E-16 | 6.54E-17 | 4.24E-17 | 2.90E-17 | 2.04E-17 |
| 890.00 | 4.55E-16 | 6.03E-17 | 3.92E-17 | 2.69E-17 | 1.89E-17 |
| 910.00 | 3.92E-16 | 5.59E-17 | 3.63E-17 | 2.49E-17 | 1.75E-17 |
| 930.00 | 4.36E-16 | 5.21E-17 | 3.37E-17 | 2.31E-17 | 1.63E-17 |
| 950.00 | 4.22E-16 | 4.84E-17 | 3.14E-17 | 2.15E-17 | 1.52E-17 |
| 970.00 | 3.48E-16 | 4.51E-17 | 2.92E-17 | 2.01E-17 | 1.42E-17 |
| 990.00 | 3.85E-16 | 4.22E-17 | 2.72E-17 | 1.87E-17 | 1.32E-17 |

dose rate at surface (rem/inc.p) as a function of distance along the beam (z,down in cm)
for tunnel-to-surface penetration of cross sectional area= 1662.00 cm2 angle w/r to beam direction= 1.57 radians
projected angle w/r to radial direction= 0.66 radians
for different lengths of penetration (in cm, across)

direct contribution

| | 405.000 | 455.000 | 505.000 | 555.000 | 605.000 |
|---|---|---|---|---|---|
| 10.00 | 0.00E+00 | 0.00E+00 | 0.00E+00 | 0.00E+00 | 0.00E+00 |
| 30.00 | 0.00E+00 | 0.00E+00 | 0.00E+00 | 0.00E+00 | 0.00E+00 |
| 50.00 | 0.00E+00 | 0.00E+00 | 0.00E+00 | 0.00E+00 | 0.00E+00 |
| 70.00 | 7.19E-25 | 5.69E-25 | 4.62E-25 | 3.83E-25 | 3.22E-25 |
| 90.00 | 4.68E-20 | 3.71E-20 | 3.01E-20 | 2.49E-20 | 2.10E-20 |
| 110.00 | 0.00E+00 | 0.00E+00 | 0.00E+00 | 0.00E+00 | 0.00E+00 |
| 130.00 | 7.73E-26 | 6.12E-26 | 4.97E-26 | 4.11E-26 | 3.46E-26 |
| 150.00 | 6.38E-19 | 5.06E-19 | 4.11E-19 | 3.40E-19 | 2.86E-19 |
| 170.00 | 1.91E-18 | 1.51E-18 | 1.23E-18 | 1.02E-18 | 8.56E-19 |
| 190.00 | 1.23E-18 | 9.73E-19 | 7.90E-19 | 6.54E-19 | 5.50E-19 |
| 210.00 | 1.92E-18 | 1.52E-18 | 1.24E-18 | 1.02E-18 | 8.62E-19 |
| 230.00 | 1.05E-17 | 8.30E-18 | 6.74E-18 | 5.58E-18 | 4.69E-18 |
| 250.00 | 1.16E-17 | 9.21E-18 | 7.48E-18 | 6.19E-18 | 5.21E-18 |
| 270.00 | 2.53E-17 | 2.01E-17 | 1.63E-17 | 1.35E-17 | 1.14E-17 |
| 290.00 | 2.65E-17 | 2.10E-17 | 1.70E-17 | 1.41E-17 | 1.19E-17 |
| 310.00 | 4.23E-17 | 3.35E-17 | 2.72E-17 | 2.25E-17 | 1.89E-17 |
| 330.00 | 4.34E-17 | 3.44E-17 | 2.79E-17 | 2.31E-17 | 1.95E-17 |
| 350.00 | 4.01E-17 | 3.18E-17 | 2.58E-17 | 2.14E-17 | 1.80E-17 |
| 370.00 | 5.46E-17 | 4.33E-17 | 3.51E-17 | 2.91E-17 | 2.45E-17 |
| 390.00 | 6.38E-17 | 5.05E-17 | 4.10E-17 | 3.40E-17 | 2.86E-17 |
| 410.00 | 4.19E-17 | 3.32E-17 | 2.70E-17 | 2.23E-17 | 1.88E-17 |
| 430.00 | 6.12E-17 | 4.85E-17 | 3.94E-17 | 3.26E-17 | 2.74E-17 |
| 450.00 | 4.99E-17 | 3.95E-17 | 3.21E-17 | 2.66E-17 | 2.24E-17 |
| 470.00 | 3.84E-17 | 3.04E-17 | 2.47E-17 | 2.04E-17 | 1.72E-17 |
| 490.00 | 3.54E-17 | 2.80E-17 | 2.27E-17 | 1.88E-17 | 1.58E-17 |
| 510.00 | 4.42E-17 | 3.50E-17 | 2.85E-17 | 2.36E-17 | 1.98E-17 |
| 530.00 | 2.95E-17 | 2.34E-17 | 1.90E-17 | 1.57E-17 | 1.32E-17 |
| 550.00 | 4.78E-17 | 3.79E-17 | 3.08E-17 | 2.55E-17 | 2.14E-17 |
| 570.00 | 3.66E-17 | 2.90E-17 | 2.35E-17 | 1.95E-17 | 1.64E-17 |
| 590.00 | 4.16E-17 | 3.30E-17 | 2.68E-17 | 2.21E-17 | 1.86E-17 |
| 610.00 | 3.69E-17 | 2.92E-17 | 2.37E-17 | 1.96E-17 | 1.65E-17 |
| 630.00 | 6.45E-17 | 5.11E-17 | 4.15E-17 | 3.43E-17 | 2.89E-17 |
| 650.00 | 4.26E-17 | 3.38E-17 | 2.74E-17 | 2.27E-17 | 1.91E-17 |
| 670.00 | 3.23E-17 | 2.56E-17 | 2.08E-17 | 1.72E-17 | 1.45E-17 |
| 690.00 | 4.35E-17 | 3.45E-17 | 2.80E-17 | 2.32E-17 | 1.95E-17 |
| 710.00 | 3.75E-17 | 2.97E-17 | 2.41E-17 | 2.00E-17 | 1.68E-17 |
| 730.00 | 3.51E-17 | 2.78E-17 | 2.26E-17 | 1.87E-17 | 1.57E-17 |
| 750.00 | 4.65E-17 | 3.69E-17 | 2.99E-17 | 2.48E-17 | 2.09E-17 |
| 770.00 | 6.33E-17 | 5.02E-17 | 4.07E-17 | 3.37E-17 | 2.84E-17 |
| 790.00 | 4.04E-17 | 3.20E-17 | 2.60E-17 | 2.15E-17 | 1.81E-17 |
| 810.00 | 3.68E-17 | 2.92E-17 | 2.37E-17 | 1.96E-17 | 1.65E-17 |
| 830.00 | 4.45E-17 | 3.53E-17 | 2.86E-17 | 2.37E-17 | 1.99E-17 |
| 850.00 | 4.06E-17 | 3.21E-17 | 2.61E-17 | 2.16E-17 | 1.82E-17 |
| 870.00 | 4.46E-17 | 3.53E-17 | 2.87E-17 | 2.37E-17 | 2.00E-17 |
| 890.00 | 4.39E-17 | 3.48E-17 | 2.82E-17 | 2.34E-17 | 1.97E-17 |
| 910.00 | 4.81E-17 | 3.81E-17 | 3.09E-17 | 2.56E-17 | 2.15E-17 |
| 930.00 | 2.47E-17 | 1.95E-17 | 1.59E-17 | 1.31E-17 | 1.11E-17 |
| 950.00 | 5.48E-17 | 4.34E-17 | 3.52E-17 | 2.92E-17 | 2.45E-17 |
| 970.00 | 4.22E-17 | 3.34E-17 | 2.71E-17 | 2.25E-17 | 1.89E-17 |
| 990.00 | 2.13E-17 | 1.69E-17 | 1.37E-17 | 1.13E-17 | 9.55E-18 |

dose rate at surface (rem/inc.p) as a function of distance along the beam (z,down in cm)
for tunnel-to-surface penetration of cross sectional area= 1862.00 cm2 angle w/r to beam direction= 1.57 radians
projected angle w/r to radial direction= 0.66 radians
for different lengths of penetration (in cm, across)

casim without penetration

| | 405.000 | 455.000 | 505.000 | 555.000 | 605.000 |
|---|---|---|---|---|---|
| 10.00 | 2.46E-16 | 1.91E-16 | 5.47E-17 | 1.92E-17 | 5.86E-18 |
| 30.00 | 2.12E-16 | 1.46E-16 | 7.44E-17 | 2.28E-17 | 7.74E-18 |
| 50.00 | 2.45E-16 | 2.40E-16 | 7.94E-17 | 2.61E-17 | 1.01E-17 |
| 70.00 | 3.23E-16 | 3.76E-16 | 9.52E-17 | 3.56E-17 | 1.22E-17 |
| 90.00 | 4.29E-16 | 3.11E-16 | 1.21E-16 | 3.76E-17 | 1.22E-17 |
| 110.00 | 6.40E-16 | 3.60E-16 | 1.40E-16 | 4.22E-17 | 1.67E-17 |
| 130.00 | 6.11E-16 | 4.35E-16 | 2.66E-16 | 7.81E-17 | 1.92E-17 |
| 150.00 | 6.35E-16 | 4.86E-16 | 2.63E-16 | 1.02E-16 | 2.74E-17 |
| 170.00 | 7.28E-16 | 5.48E-16 | 2.63E-16 | 6.90E-17 | 2.21E-17 |
| 190.00 | 9.91E-16 | 7.03E-16 | 2.76E-16 | 8.46E-17 | 3.01E-17 |
| 210.00 | 1.09E-15 | 8.92E-16 | 3.21E-16 | 1.21E-16 | 3.24E-17 |
| 230.00 | 1.71E-15 | 1.50E-15 | 3.40E-16 | 1.11E-16 | 4.26E-17 |
| 250.00 | 1.42E-15 | 1.36E-15 | 3.47E-16 | 1.22E-16 | 6.33E-17 |
| 270.00 | 1.63E-15 | 1.48E-15 | 5.00E-16 | 1.40E-16 | 6.91E-17 |
| 290.00 | 1.37E-15 | 1.30E-15 | 5.15E-16 | 3.25E-16 | 6.52E-17 |
| 310.00 | 1.58E-15 | 1.26E-15 | 4.78E-16 | 6.41E-16 | 1.43E-16 |
| 330.00 | 1.79E-15 | 1.23E-15 | 8.22E-16 | 2.11E-16 | 1.13E-16 |
| 350.00 | 2.25E-15 | 1.44E-15 | 6.19E-16 | 2.31E-16 | 8.86E-17 |
| 370.00 | 1.97E-15 | 1.59E-15 | 4.80E-16 | 4.68E-16 | 1.10E-16 |
| 390.00 | 2.30E-15 | 1.59E-15 | 5.35E-16 | 3.39E-16 | 1.31E-16 |
| 410.00 | 2.30E-15 | 2.05E-15 | 8.25E-16 | 3.00E-16 | 1.07E-16 |
| 430.00 | 2.52E-15 | 1.76E-15 | 1.11E-15 | 3.65E-16 | 1.11E-16 |
| 450.00 | 2.96E-15 | 1.86E-15 | 8.97E-16 | 3.73E-16 | 9.13E-17 |
| 470.00 | 3.18E-15 | 2.19E-15 | 7.99E-16 | 8.49E-16 | 1.40E-16 |
| 490.00 | 3.39E-15 | 2.11E-15 | 8.85E-16 | 4.20E-16 | 1.47E-16 |
| 510.00 | 2.89E-15 | 2.27E-15 | 8.95E-16 | 3.38E-16 | 1.70E-16 |
| 530.00 | 3.13E-15 | 2.47E-15 | 1.40E-15 | 3.79E-16 | 1.20E-16 |
| 550.00 | 3.15E-15 | 2.30E-15 | 7.84E-16 | 4.68E-16 | 1.80E-16 |
| 570.00 | 2.53E-15 | 2.16E-15 | 9.69E-16 | 4.98E-16 | 1.37E-16 |
| 590.00 | 2.57E-15 | 2.78E-15 | 7.56E-16 | 4.53E-16 | 1.03E-16 |
| 610.00 | 2.70E-15 | 2.62E-15 | 9.44E-16 | 2.46E-16 | 1.31E-16 |
| 630.00 | 2.53E-15 | 2.09E-15 | 8.09E-16 | 3.05E-16 | 1.17E-16 |
| 650.00 | 2.37E-15 | 1.86E-15 | 1.20E-15 | 2.74E-16 | 1.04E-16 |
| 670.00 | 2.28E-15 | 2.64E-15 | 9.08E-16 | 3.65E-16 | 1.17E-16 |
| 690.00 | 1.90E-15 | 2.25E-15 | 8.12E-16 | 3.63E-16 | 1.33E-16 |
| 710.00 | 3.05E-15 | 2.17E-15 | 7.03E-16 | 3.22E-16 | 1.48E-16 |
| 730.00 | 2.48E-15 | 1.76E-15 | 5.50E-16 | 2.34E-16 | 8.34E-17 |
| 750.00 | 2.52E-15 | 1.70E-15 | 5.10E-16 | 2.05E-16 | 6.96E-17 |
| 770.00 | 2.30E-15 | 1.61E-15 | 5.45E-16 | 2.17E-16 | 7.02E-17 |
| 790.00 | 1.75E-15 | 1.48E-15 | 5.88E-16 | 2.88E-16 | 7.28E-17 |
| 810.00 | 2.09E-15 | 1.51E-15 | 5.60E-16 | 2.44E-16 | 3.70E-16 |
| 830.00 | 1.56E-15 | 1.11E-15 | 7.20E-16 | 1.84E-16 | 1.11E-16 |
| 850.00 | 1.18E-15 | 1.25E-15 | 4.74E-16 | 3.39E-16 | 1.43E-16 |
| 870.00 | 1.36E-15 | 1.16E-15 | 4.62E-16 | 2.29E-16 | 7.44E-17 |
| 890.00 | 1.23E-15 | 1.26E-15 | 4.34E-16 | 1.40E-16 | 8.18E-17 |
| 910.00 | 1.43E-15 | 1.12E-15 | 4.44E-16 | 1.82E-16 | 5.19E-17 |
| 930.00 | 1.44E-15 | 8.21E-16 | 2.71E-16 | 1.68E-16 | 4.66E-17 |
| 950.00 | 1.35E-15 | 9.46E-16 | 2.80E-16 | 1.94E-16 | 5.81E-17 |
| 970.00 | 8.83E-16 | 9.67E-16 | 3.12E-16 | 1.84E-16 | 4.62E-17 |
| 990.00 | 1.03E-15 | 7.61E-16 | 5.90E-16 | 7.84E-17 | 4.74E-17 |

dose rate at surface (rem/inc.p) as a function of distance along the beam (z,down in cm)
for tunnel-to-surface penetration of cross sectional area= 1662.00 cm2 angle w/r to beam direction= 1.57 radians
projected angle w/r to radial direction= 0.66 radians
for different lengths of penetration (in cm, across)

total

| | 405.000 | 455.000 | 505.000 | 555.000 | 605.000 |
|---|---|---|---|---|---|
| 10.00 | 8.12E-15 | 3.75E-15 | 2.43E-15 | 1.62E-15 | 1.09E-15 |
| 30.00 | 9.09E-15 | 4.22E-15 | 2.79E-15 | 1.86E-15 | 1.25E-15 |
| 50.00 | 1.06E-14 | 4.91E-15 | 3.18E-15 | 2.12E-15 | 1.43E-15 |
| 70.00 | 1.32E-14 | 5.66E-15 | 3.59E-15 | 2.39E-15 | 1.61E-15 |
| 90.00 | 1.68E-14 | 6.22E-15 | 4.01E-15 | 2.66E-15 | 1.80E-15 |
| 110.00 | 2.11E-14 | 6.89E-15 | 4.41E-15 | 2.92E-15 | 1.99E-15 |
| 130.00 | 2.29E-14 | 7.36E-15 | 4.79E-15 | 3.13E-15 | 2.12E-15 |
| 150.00 | 2.49E-14 | 7.69E-15 | 4.95E-15 | 3.27E-15 | 2.21E-15 |
| 170.00 | 2.92E-14 | 8.06E-15 | 5.13E-15 | 3.36E-15 | 2.30E-15 |
| 190.00 | 3.19E-14 | 8.38E-15 | 5.21E-15 | 3.42E-15 | 2.35E-15 |
| 210.00 | 3.41E-14 | 8.53E-15 | 5.21E-15 | 3.42E-15 | 2.33E-15 |
| 230.00 | 3.71E-14 | 8.97E-15 | 5.08E-15 | 3.32E-15 | 2.28E-15 |
| 250.00 | 3.84E-14 | 8.53E-15 | 4.88E-15 | 3.18E-15 | 2.20E-15 |
| 270.00 | 3.80E-14 | 8.35E-15 | 4.83E-15 | 3.07E-15 | 2.12E-15 |
| 290.00 | 3.74E-14 | 7.88E-15 | 4.65E-15 | 3.12E-15 | 2.03E-15 |
| 310.00 | 3.87E-14 | 7.49E-15 | 4.36E-15 | 3.28E-15 | 1.99E-15 |
| 330.00 | 4.01E-14 | 7.16E-15 | 4.48E-15 | 2.88E-15 | 1.85E-15 |
| 350.00 | 3.94E-14 | 7.01E-15 | 4.05E-15 | 2.54E-15 | 1.72E-15 |
| 370.00 | 3.91E-14 | 6.78E-15 | 3.65E-15 | 2.61E-15 | 1.62E-15 |
| 390.00 | 3.99E-14 | 6.49E-15 | 3.51E-15 | 2.34E-15 | 1.54E-15 |
| 410.00 | 3.54E-14 | 6.59E-15 | 3.58E-15 | 2.15E-15 | 1.41E-15 |
| 430.00 | 3.34E-14 | 5.97E-15 | 3.68E-15 | 2.09E-15 | 1.33E-15 |
| 450.00 | 3.89E-14 | 5.95E-15 | 3.35E-15 | 2.02E-15 | 1.26E-15 |
| 470.00 | 4.40E-14 | 6.07E-15 | 3.09E-15 | 2.37E-15 | 1.21E-15 |
| 490.00 | 4.00E-14 | 5.72E-15 | 3.01E-15 | 1.83E-15 | 1.14E-15 |
| 510.00 | 3.61E-14 | 5.72E-15 | 2.93E-15 | 1.69E-15 | 1.12E-15 |
| 530.00 | 3.29E-14 | 5.62E-15 | 3.26E-15 | 1.62E-15 | 9.97E-16 |
| 550.00 | 3.13E-14 | 5.30E-15 | 2.58E-15 | 1.65E-15 | 1.01E-15 |
| 570.00 | 3.14E-14 | 5.02E-15 | 2.64E-15 | 1.61E-15 | 9.18E-16 |
| 590.00 | 3.05E-14 | 5.42E-15 | 2.29E-15 | 1.47E-15 | 8.18E-16 |
| 610.00 | 3.16E-14 | 5.02E-15 | 2.38E-15 | 1.20E-15 | 7.98E-16 |
| 630.00 | 2.78E-14 | 4.35E-15 | 2.13E-15 | 1.18E-15 | 7.38E-16 |
| 650.00 | 2.27E-14 | 3.86E-15 | 2.37E-15 | 1.05E-15 | 6.55E-16 |
| 670.00 | 2.04E-14 | 4.54E-15 | 2.01E-15 | 1.09E-15 | 6.30E-16 |
| 690.00 | 1.93E-14 | 4.06E-15 | 1.87E-15 | 1.07E-15 | 6.29E-16 |
| 710.00 | 2.36E-14 | 3.94E-15 | 1.73E-15 | 9.98E-16 | 6.25E-16 |
| 730.00 | 2.12E-14 | 3.41E-15 | 1.50E-15 | 8.61E-16 | 5.25E-16 |
| 750.00 | 1.71E-14 | 3.16E-15 | 1.36E-15 | 7.70E-16 | 4.70E-16 |
| 770.00 | 1.57E-14 | 2.95E-15 | 1.33E-15 | 7.41E-16 | 4.43E-16 |
| 790.00 | 1.42E-14 | 2.71E-15 | 1.31E-15 | 7.70E-16 | 4.16E-16 |
| 810.00 | 1.67E-14 | 2.72E-15 | 1.27E-15 | 7.14E-16 | 7.03E-16 |
| 830.00 | 1.50E-14 | 2.28E-15 | 1.41E-15 | 6.40E-16 | 4.34E-16 |
| 850.00 | 1.22E-14 | 2.38E-15 | 1.13E-15 | 7.75E-16 | 4.51E-16 |
| 870.00 | 1.15E-14 | 2.22E-15 | 1.08E-15 | 6.43E-16 | 3.68E-16 |
| 890.00 | 9.99E-15 | 2.23E-15 | 1.00E-15 | 5.22E-16 | 3.54E-16 |
| 910.00 | 1.01E-14 | 2.00E-15 | 9.64E-16 | 5.30E-16 | 2.99E-16 |
| 930.00 | 9.16E-15 | 1.62E-15 | 7.33E-16 | 4.75E-16 | 2.63E-16 |
| 950.00 | 9.22E-15 | 1.76E-15 | 7.55E-16 | 5.12E-16 | 2.86E-16 |
| 970.00 | 8.90E-15 | 1.71E-15 | 7.45E-16 | 4.73E-16 | 2.53E-16 |
| 990.00 | 1.00E-14 | 1.42E-15 | 9.67E-16 | 3.28E-16 | 2.24E-16 |

K+E 10 X 10 TO ½ INCH 7 X 10 INCHES KEUFFEL & ESSER CO. MADE IN U.S.A. 46 1320

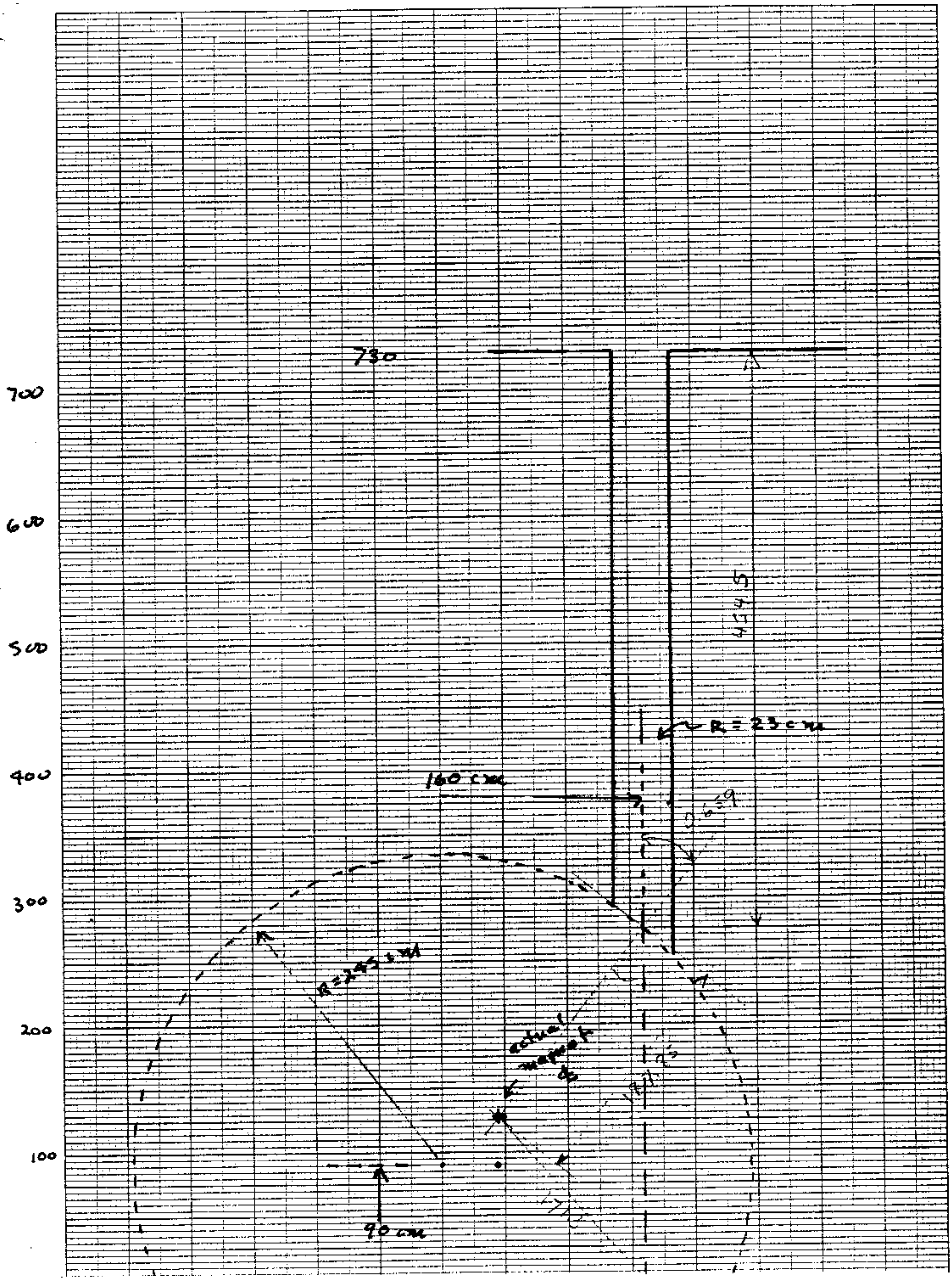

**Brookhaven National Laboratory**

**MEMORANDUM**

Date: 08/23/96

To: S. Musolino

From: A.J. Stevens AJS

Subj.: Fence Locations Around Cryogenic Bypass Holes

Most interaction regions have relatively large holes in the berm cover through which cryogenic pipes pass to "bridge" the experimental areas. Since a fault near such a hole can produce a large dose on top of the berm, access must be restricted from regions near which these pipes exit or enter the berm. Presumably fences of appropriate characteristics will provide this access restriction. This memorandum describes a procedure for locating these fences with the bypass at 6 o'clock taken a specific case.

The dose emerging from the hole is (once again) considered to have both "high" and "low" energy components. The high energy component is dose from high energy hadrons (> CASIM threshold) that either emerge through the hole or which interact in the berm close to the hole. The low energy component is dose from neutrons that "percolate through" the hole.

The fall off of the low energy component can be estimated by the same procedure used to estimate the fall off of excess dose from the exit of vent shafts[1] (where the low energy dose is the only significant component). The first step is to calculate the value of this component at the exit of the hole. Here I treat the shaft as the first leg of a labyrinth and use the entrance dose from the calculation of Ref [1] evaluated at a distance from the beam line of 9.83 ft, which corresponds to the situation at 6 o'clock. Since the high $\beta$ quads are in this region, the loss must be considered to be the full $2.28 \times 10^{13}$ protons. The entrance dose is 401 rem.

The hole at 6 o'clock is 2 ft in the beam direction by 5 ft. laterally, and the distance through the berm is (the usual) 13 ft. This gives a universal length ($d = L/\sqrt{A}$) of 4.11. Applying Goebel's first length attenuation to the 401 rem gives 6.4 rem at the exit of the hole. Now the 4.11 is (by fortuitous coincidence) very close to one of the values for which the angular dependence of neutrons was calculated by Vogt.[2] The attachment to this memorandum reproduces Fig. 13 of Ref. [1],(where a smooth curve has been added over the histogram at $d$=4.41).

The situation is sketched in Fig. 1 below which shows the canonical 6 ft. tall person standing some distance D away from the exit of the hole.

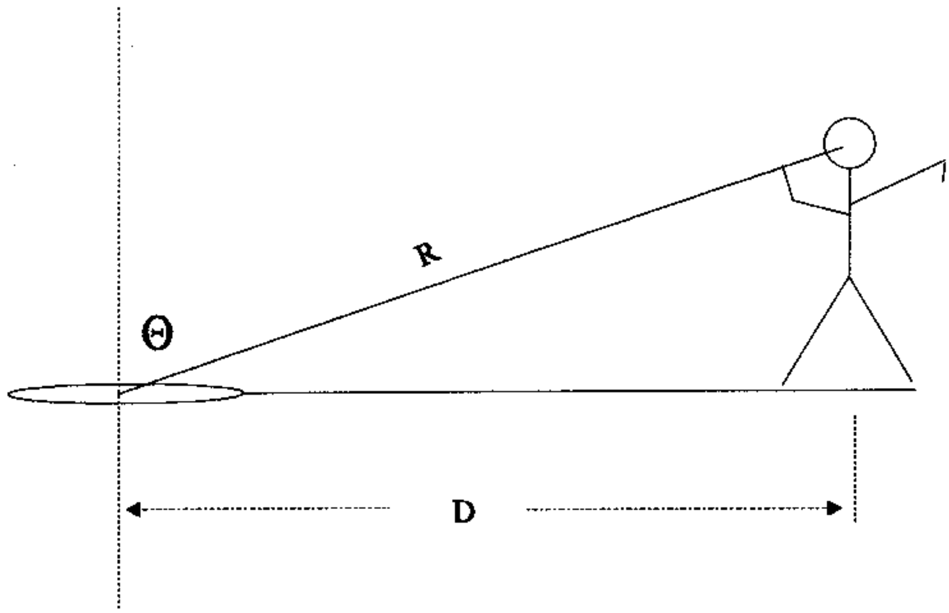


Fig. 1 Illustrating the Low Energy Calculation

Assuming the stick figure is far enough away from the hole that variations across the hole itself can be ignored, the reduction factor at some distance R is given by:

$$RF = \frac{10ft^2 \times f(\Omega)}{R^2 \times \int f(\Omega)d\Omega}$$

where $f$ is simply read from the attachment at any polar angle (which increases as the person moves away) and the integral in the denominator is simply the sum of the values shown (1.85 for d=4.14 in the attachment). [The 10 $ft^2$ is just the hole area at 6 o'clock].

Now this formula will give a finite excess dose at the moon for example, so one needs some target value for the reduction factor. I have recently made a cursory examination of all the o'clock locations near the high β quads. At 6 o'clock the dose, ignoring the hole, was 112 mrem. This is in part because the distance from the beam line is reasonably large here, so the 13 ft. of earth is sufficient. There is margin for 160 - 112 = 48 mrem excess. Somewhat arbitrarily, I assign half of this margin for the low energy component which gives the desired reduction factor, namely 24 mrem/6.4 rem = $3.75\times10^{-3}$. This is achieved at D = 12 ft. [Note that this distance could be several feet shorter if the 13 ft. berm were increased.]

The high energy part is now considered. Except very near the hole (where evaporation neutrons created near the sides of the hole "percolate out") the high energy component is dominated by punch through.

The situation is illustrated in Fig. 2 below.

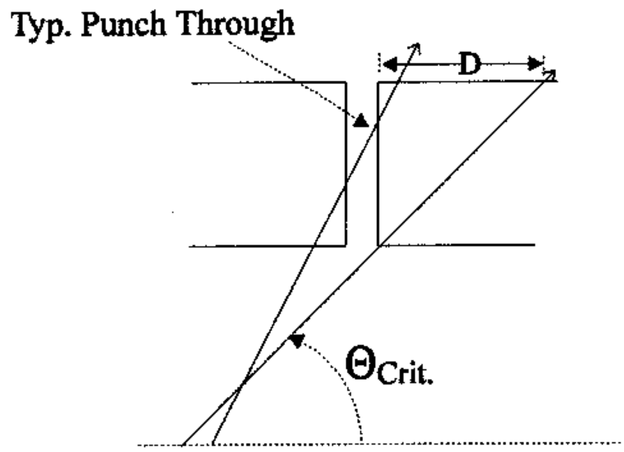


Fig. 2. Illustration of the High Energy Estimate

We first consider the following crude argument. In the beam direction the high energy dose is "forward." In CASIM (in this geometry), the star density maximum on the surface is at an angle of 50° with respect to the beam line. [There is some evidence that the CASIM angles are more forward than actually observed which makes the estimate here too conservative.] Now the hole reduces the earth shielding by $L/\cos(\theta)$ where L in the length of the hole (2 ft at 6 o'clock) for any angle $\theta$ drawn from the interior to the surface. The path length through earth is:

$$\frac{13ft}{\sin(\Theta)} - \frac{2ft}{\cos(\Theta)}$$

Now at some "critical" value of $\Theta$ this path is greater than the path through solid earth at the star density maximum value (50°). This turns out to be 41°. When the ray at this angle is aligned at the edge of the hole, as shown in Fig. 2, the excess punch through should be reduced to a small value. This gives D = 15 ft. in Fig. 2.

Now this argument cannot be correct in detail since it treats the hadron cascade as if it were a single "average" particle. To "test" the argument I performed two CASIM calculations. In the first a 2 ft. long empty slot in a 13 ft. thick shield was put in the shield at a position relative to loss on a quadrupole that I simply guessed was the worst case. This was compared a second calculation where the shield was solid. The two calculations were compared to find what distance downstream of the slot gave the same star density as the maximum star density in the no-slot calculation. The result was a distance between 16 and 17 ft. which agrees well with the geometric argument. One should allow a little safety here, so 20 ft. is chosen.

In the transverse direction, the simple geometric argument gives a very limited extent since all punch through "rays" are simply radial lines. In this direction, the low energy distance dominates.

For the low energy component the width of the hole should be added to the 12 ft., **so a fence at ±20 ft. in the beam direction by ±14 ft. in the transverse direction should be sufficient**.

The method described herein can be applied to locations other than 6 o'clock, but not the conclusion. The 6 o'clock location has a 3 ft. concrete roof which helps reduce the dose. Each location must be examined separately.

## References


1. A.J. Stevens, "Radiation Field in the Vicinity of the Collider Center," AD/RHIC/RD-77, October, 1994.

2. H.G. Vogt, "Monte Carlo Calculations of the Neutron Transmission Through the Access Ways of the CERN Super Proton Synchrotron," CERN 75-14 (1975).


Attachment

ATTACHMENT
- FROM REF. [1]

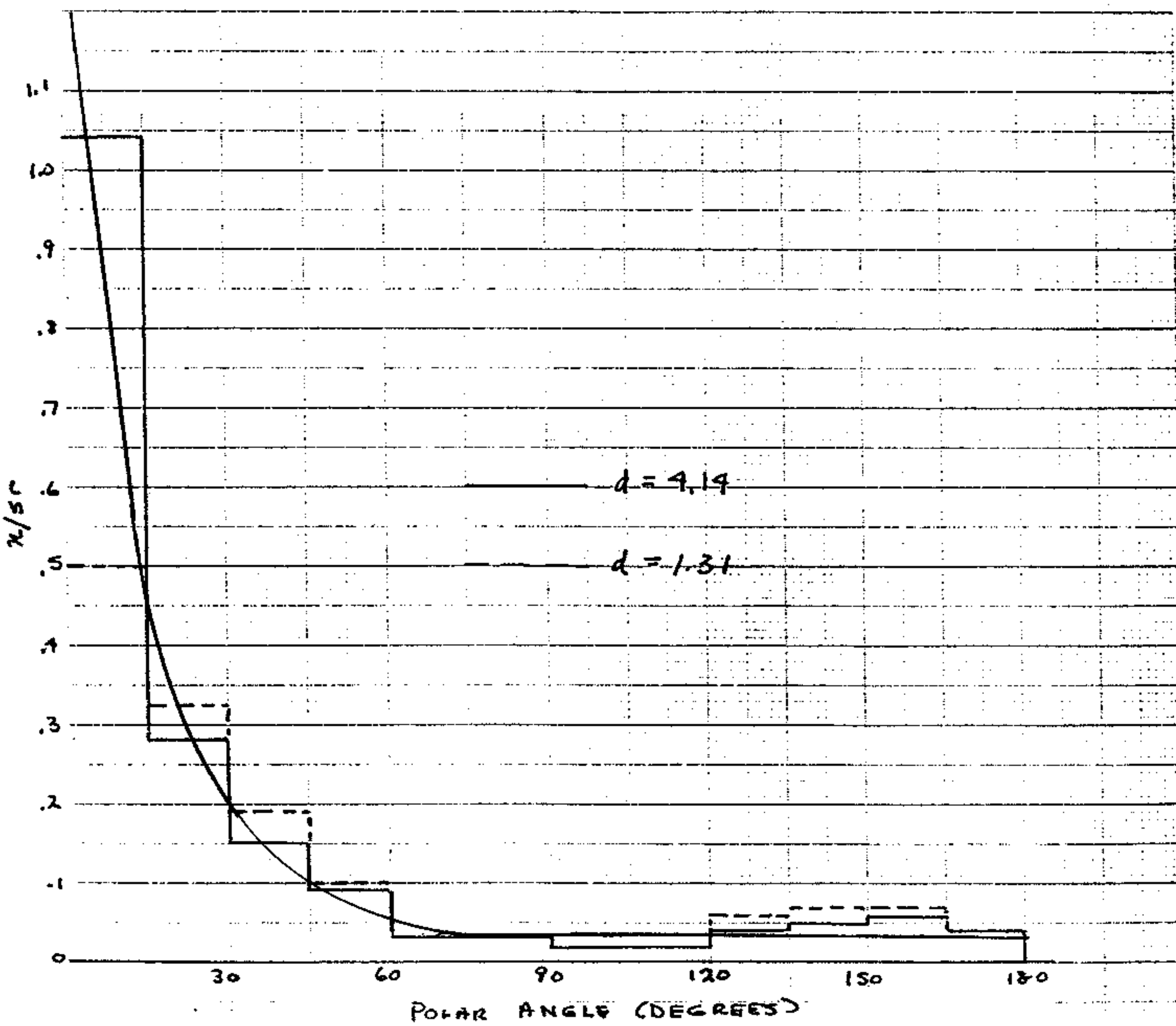


Fig. 13 Neutron Direction vs. Universal Length
Adapted from Fig. 9 of Ref. [15]